Magnetic Resonance Imaging Velocimetry of Fluid Flow in a Clinical Blood Filter

Frank Heese, Philip Robson, and Laurie Hall
Herchel Smith Laboratory for Medicinal Chemistry (HSLMC), University of Cambridge School of Clinical Medicine, Cambridge CB2 2PZ, U.K.

DOI 10.1002/aic.10504
Published online June 13, 2005 in Wiley InterScience (www.interscience.wiley.com).

Multislice spin echo (SE) pulsed-field gradient phase-contrast (PFG-PC) magnetic resonance imaging (MRI) velocimetry has been used to determine the complex three-dimensional (3-D) recirculatory flow pattern of a simple, single-phase blood analogue fluid (glycerol–water solution 70–30 vol%) in a commercially available blood filter (PALL AL8 arterial line blood filter), whose inlet and outlet ports are about 0.95 cm in diameter. The maximum shear stress measured in the fluid is 10 Pa, which is significantly lower than the value for the onset of red blood cell hemolysis. The flow field is in agreement with computational flow modeling (Fluent 4.3) and is reminiscent of the hydrocyclone flow in industrial separation devices. The development of this flow pattern is demonstrated for three different volume flow rates (1, 2, and 3 L/min). © 2005 American Institute of Chemical Engineers *AIChE J,* 51: 2396–2401, 2005
Keywords: magnetic resonance imaging velocimetry, complex flow pattern, arterial line blood filter, shear stress, hydrocyclone flow

Introduction

It is already well known among magnetic resonance imaging (MRI) specialists that MRI velocimetry based on the responses from the protons in the fluid is uniquely capable of determining in three dimensions the entire 3-D-vector flow field of optically opaque, rheologically complex fluids in geometrically convoluted flow systems.[1-5] The present study of the commercially available PALL AL8 arterial line blood filter is intended to demonstrate to an engineering audience the potential of these techniques. The MRI measurements clearly demonstrate that the flow field of a simple blood analogue fluid in this filter follows a complex recirculatory pattern that could not have been determined using other velocimetric methods. Moreover, it demonstrates that MRI velocity data can be used to gain further insight into the system by using the velocity field to calculate, first the shear strain rate field, and then the shear stress field, throughout the fluid. These findings will be of interest not only to those involved with filtration and medical devices, but also, more generally, to fluid dynamics researchers or process engineers who may infer opportunities to investigate new fluids, or new velocimetric measurements of previously inaccessible systems.

The PALL AL8 arterial line blood filter is designed for extracorporeal use in heart-bypass operations to filter the blood before reperfusion into the patient. It is designed to remove small air emboli introduced during aeration of the blood, system particulates, and solidus thrombi of clotted blood or arterial plaques. The thrombi result from contact of the blood with nonbiological material or the stresses it undergoes during the operation, whereas the plaques are dislodged from the arteries during the surgical procedure. If such air or particulate emboli enter the patients' blood stream they can cause occlusions in the vasculature, potentially leading to stroke and/or brain damage.

Determination of the flow field allows assessment of the filter usage and the path of the fluid before it enters into the filter medium. These factors are important because they can affect the shear stresses on the red blood cells; the time blood cells spend in the filter and therefore outside the body; and whether there are areas of underused filter medium. Minimizing the shear stress is

Correspondence concerning this article should be addressed to L.D. Hall at ldh11@hslmc.cam.ac.uk.

important for limiting the potential damage to the blood cells and, therefore, both the production of dangerous embolic debris and the loss of essential oxygen-carrying material.

Although there are several excellent texts[6-8] that provide full details of the MRI method, a brief introduction is given here to facilitate the subsequent discussions of this study. Most MRI measurements are based on the responses obtained from the nuclei of the hydrogen protons of fluids (such as water and hydrocarbons) in vessels or materials when bathed with pulses of a homogeneous magnetic field at the appropriate radiofrequency.

The spatial distribution of that fluid can be measured in one (1-D), two (2-D), or three dimensions (3-D) by using the appropriate combination of three orthogonally oriented magnetic field gradients, each of which induces a spatially related distribution of the proton resonance frequencies.

For example, a single field gradient applied in the vertical orientation will give the top-to-bottom distribution of the protons. More productively, simultaneous application of a matrix of two, mutually orthogonal gradient fields leads to a 2-D slice distribution; ultimately a set of three orthogonal gradients gives a full 3-D image matrix that can be subsequently viewed as a series of 2-D-slice images oriented at any direction to the structure of the sample. Although the relative intensities of the individual pixels in all such images depend on the scan protocol used, in most cases they relate directly to the concentration of the fluid.

Pulses of those same magnetic field gradients, applied to the sample before those used to visualize the spatial structures, induce variations in the response signals that depend on the flow velocity of the fluid. For example, for a fluid flowing along a round pipe, application of gradient pulses parallel to the long axis of the pipe lead to a cross-sectional image of the distribution of flow velocities in the plane perpendicular to the pipe axis. In the present studies of flow in a vertically oriented cylindrical vessel, a scan protocol was developed that provides a parallel set of 2-D-slice images oriented horizontally. The flow through, and within, all those planes was then measured. Importantly, those images distinguish between upward and downward flow, and thus measurements of the flow velocity vectors are made.

To the best of our knowledge MRI is the only method that can measure the complete 3-D distribution of flow velocities for an optically opaque fluid. Although the fact that the fluid must have detectable proton MRI responses, and be contained in a vessel that is transparent to magnetic and radiofrequency fields, excludes many direct applications to industrial processes, nevertheless many systems are suitable. In particular, many of the devices used in clinical surgery are intentionally fabricated from plastic and are metal-free. Furthermore, the relevant fluids, either blood, or water-based plasma extenders, all provide sufficiently high intensity MRI responses, which all the above measurement protocols can be made to provide high spatial resolution images.

Experimental

The AL8 filter, shown in Figure 1, has a cylindrical geometry; in-flow is through a horizontal port tangential to the top and on the edge of the device, and out-flow is through a central, vertical port at the base. Blood enters the outer cylindrical annular cavity; passes through the woven filter medium, which is itself pleated into a cylindrical annular shape; and from there into the central cylindrical core. To remove any larger air bubbles that may inadvertently arise in the system a small volume of blood is continuously drawn off (and returned to the bypass system) through a small outlet port centrally mounted on the top of the filter. The filter is made entirely from plastics (polycarbonate body and polyester filtration media) and is thus ideally suited to MRI studies. The device has approximate dimensions of 7.5 cm (diameter) $\times$ 7.5 cm (height); the in-flow and out-flow ports are about 0.95 cm in diameter. The filter is designed for a mean operating flow rate of 4–5.5 L/min, which is required to match the cardiac output of the heart, and can operate up to a maximum of 8 L/min.

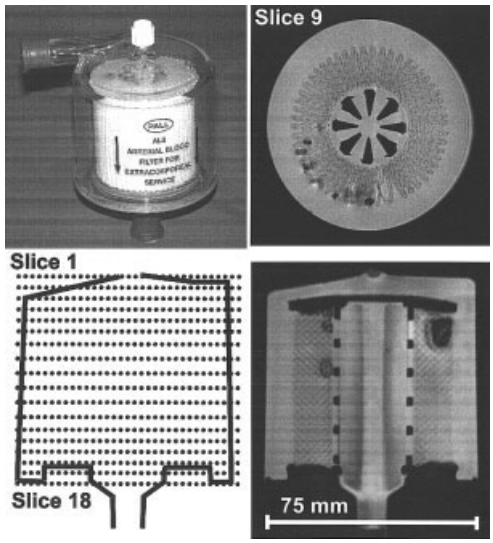

Figure 1. Top left: Photograph of the PALL AL8 arterial line blood filter for extracorporeal use; blood enters from the horizontal inlet port on the top of the filter body and exits through the central vertical outlet port at the base; the filter medium (white) is pleated into a cylindrical annular formation; fluid is bled through the vent line port on the top of the filter to remove small air bubbles that have entered the vessel; top and bottom right: 2-D slice MR images of static 10 mM aqueous copper sulfate solution (which facilitates reduction of the scan time required) in a PALL AL8 filter showing the internal structures of the filter; fluid appears bright and plastic or air inclusions appear black; bottom left: positions of the transverse slices (1–18) in which the flow velocities were subsequently measured; slice 9 is shown top right.

Images were obtained using a standard 2-D gradient echo-imaging protocol (GEFI) with TR 200 ms, TE 9 ms, flip angle 90°, FOV/matrix 12 $\times$ 12 cm/512 $\times$ 512 giving an isotropic in-plane resolution of 234 μm, and a slice thickness of 3.05 mm. A total of eight averages were taken in about 14 min.

The MRI system consisted of a 2-T, 100-cm bore, Oxford Instruments superconducting magnet, interfaced with a Medspec AVANCE console (Bruker Medizin Technik GmbH, Karlsruhe, Germany), operating under Paravision 2.1.1 software. The gradient set was 24 cm diameter and 40 mT/m maximum strength, and a sine-space probe of 17 cm diameter was used; both were made at the HSLMC.

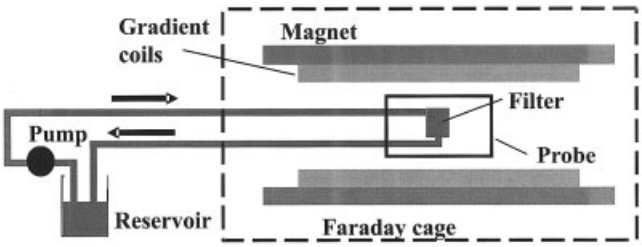

Figure 2. Flow rig showing the filter (7.5 cm diameter) mounted in the probe (17 cm diameter), inside the magnet (100 cm diameter bore); and the fluid reservoir and gear pump used to supply a steady fluid flow; long PVC pipes (0.95 cm diameter, length about 10 m) required to connect the pump/reservoir to the filter from well outside the Faraday cage (~5 m away).

A cradle was manufactured from Perspex® to hold the filter firmly in place in the radiofrequency (RF) probe. Long polyvinylchloride pipes (0.95 cm diameter, length about 10 m) were required to supply fluid to the filter inside the magnet from a reservoir and pump set up outside the Faraday cage that surrounds the MRI scanner (Figure 2). A gear pump (Micropump Inc., IDEX Corp., Vancouver, WA) was used to provide a steady flow at rates of up to 3 L/min.

Static imaging was carried out with a separate identical filter filled with 10 mM aqueous copper sulfate solution (which facilitates reduction of the scan time required), using a standard 2D gradient echo-imaging protocol (GEFI), with isotropic in-plane resolution of 234 μm in about 14 min.

The blood analog fluid used for the flow measurements, in accordance with the manufacturer's testing, is a simple Newtonian fluid: 70 vol % glycerol (Rectapur 98% glycerol, Merck Eurolab Ltd.), 30 vol % distilled water; a small amount of surfactant solution (0.1% Triton-X 100, BDH Laboratory Supplies, Poole, UK) was also added. The fluid was chosen to match the viscosity of normal undiluted blood: the density (ρ) was 1.18 g/cm^3 and viscosity (η) was 0.018 Pa·s (18.0 cP) at room temperature. Based on Poiseuille flow in the inlet pipe, of diameter $D = 0.95$ cm, at a flow rate of 2 L/min, with a maximum velocity, $v = 94$ cm/s, the system has a Reynolds number (Re) of 585, given by the following equation

$$\mathrm{Re} = \frac{\rho v D}{\eta} = 585 \qquad (1)$$

At this value the flow pattern developed is expected to be steady and laminar.[9]

The flow velocities were measured using a phase-contrast, pulsed-field gradient, multislice, spin-echo imaging sequence[2,6]; 18 parallel slice images were obtained. All parameters were set to minimize the TE, equal to 9.9 ms, to limit fluid motion between excitation and acquisition. Gaussian-shaped RF pulses were used to minimize the duration of the pulses; the dwell time was set to 10 μs, and further reduction was considered too disadvantageous because of the increased noise associated with a wider spectral width of the signal. The sequence is run three times, once for each component of the velocity vector, with the velocity encoding gradients applied in the slice-, read-, and phase-encode directions. The phase shift in each image, arising from fluid motion, is found by subtracting the phase image of a reference image acquired with the same velocity encoding sequence but no flow in the system. The total scan time to acquire the complete 3-D velocity field is about 3 h.

Data processing uses CaMReS software.[10] The velocity is calculated from the variation of phase shift with velocity encoding gradient strength on a pixel-by-pixel basis using a Bayesian analysis technique, written by members of the HSLMC,[11] which takes into account the signal-to-noise ratio of the image. Velocity maps are then processed further, and visualized, using the Matlab toolbox (Matlab 6.5, The MathWorks, Natick, MA) to mask erroneous noise, recombine the three orthogonal components of velocity, and add velocity vectors.

Results and Discussion

Static imaging

The static images, shown in Figure 1, clearly delineate the internal structures of the filter, that is, the pleated form of the filter medium, the diagonal pattern of the support meshing that holds the filter medium in place, the shape of the annular cavity with the fluid-filled space above the solid plastic (dark) molding at the top of the filter medium, and the structure of the central outlet cavity showing solid plastic fins. In addition, Figure 1 shows the presence of air bubbles trapped on the filter medium; they appear as dark voids with a characteristic pattern of light and dark regions surrounding them.[12] These bubbles are a result of imperfect priming of the filter and, for flow imaging, a superior priming procedure closer to the standard clinical procedure was followed and virtually no bubbles were then evident; any that did remain stayed trapped on the filter during flow imaging and did not interfere with the measurements. Figure 1 also shows the positions of the 18 slices for which velocity measurements were subsequently made.

Velocimetry

Velocity imaging measurements were repeated several times on different days, with a fresh filter on each occasion, and a completely new imaging session on the scanner; this was done to demonstrate the repeatability of the findings, which is of particular importance in the medical devices field where quality control is imperative. No significant difference was found between any of the resultant velocity images; the flow patterns were qualitatively identical, and the peak flow velocity showed $<10\%$ difference between successive scans, which is within the expected variance for MRI velocimetry. It is known[11,13] that MRI phase-contrast velocimetry methods such as that used here typically measure velocities with a precision of a few percent, based, as they are, on a measurement of the phase of the signal. As a result, measured flow profiles across a vessel agree very well with analytical flow profiles, such as Poiseuille flow in a straight tube.

The set of 18 slice images taken across the body of the filter, shown in Figure 3 (slices 1 and 18 omitted), show the flow field in the annular cavity of the filter body for a flow rate of 2 L/min, which corresponds to a Reynolds number in the inlet pipe of 585. A downward-moving submerged jet is clearly seen after the tangential entry inlet port, which spreads out against the vessel walls and spirals around the annular cavity as it

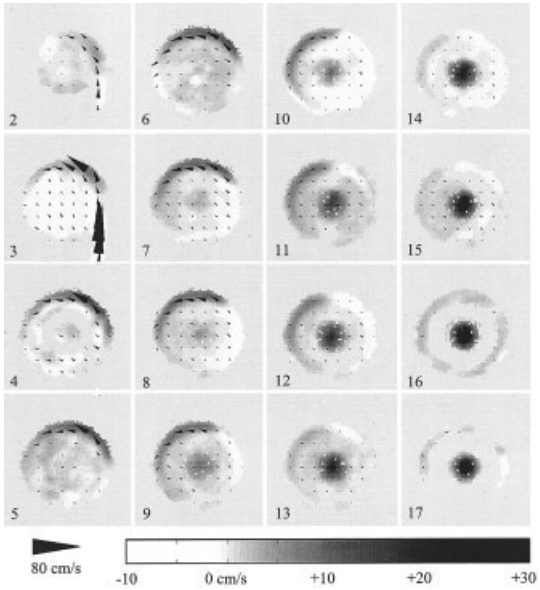

Figure 3. MRI velocimetry measurements, in units of cm/s, for the blood analog fluid in an AL-8 filter at a flow rate of 2 L/min.

Slices 2–17 are consecutive slices across the filter from top to bottom and correspond to those shown in Figure 1. Tonal value represents through-plane flow; dark, positive velocities corresponding to vertical downward flow from top to bottom, and white negative values corresponding to vertical upward flow; in-plane flow velocity direction is represented by cone vectors, whose length represents flow speed. These maps clearly show the downward spiraling inlet jet and a recirculatory upward moving body of fluid. The data set consists of 18 parallel slice images obtained in three sets, each of six slices; the slice separation for the top section around the inlet port and for the bottom section around the outlet was 3.0 mm; for the main body it was 5.5 mm. The slice thickness was 1.5 mm for all slices and the 1.5 mm in-plane resolution was achieved using a 128 × 128 matrix and a 19.2-cm-square field of view. The recovery time and echo time, TR/TE, were 2000/9.9 ms. The time interval between the velocity encoding gradient pulses (Δ) was 5.4 ms, each pulse having a duration (δ) of 0.4 ms; seven gradient strength steps were used, evenly spaced from 0 to 6 mT/m.

descends. Importantly, it remains intact until it reaches the bottom of the cavity where its vertical momentum is reversed, leading to an upwardly spiraling body of fluid; the resultant recirculatory flow pattern in the annular cavity is clearly detected. Because the momentum of the initial jet carries the descending fluid to the outer edge of the cylindrical cavity, it is the rising fluid that contacts, and passes through, the filter medium mounted cylindrically in the center of the filter.

Shear stress calculations

The aspect of the flow pattern that is of major concern to the design of blood filters is the shear stresses imposed on the red blood cells, especially at the entry and exit points in the filter where the gradients of the flow velocity profile are greatest; fortunately, analysis of such shear stresses is possible using 3-D MRI velocity data. The shear strain rate field is derived, on a pixel-by-pixel basis, by calculating the changes in velocity between adjacent pixels in the 3-D matrix of velocity data $\boldsymbol{v}(x, y, z)$, at each point in space (x, y, z), in both directions in-plane, and also between adjacent slices in space. The shear stress tensor $S_{ij}(x, y, z)$ is subsequently calculated, given a priori knowledge of the fluid shear-viscosity η based on the tensor equation, as

$$S_{ij} = \eta\left(\frac{dv_i}{dx_j} + \frac{dv_j}{dx_i}\right) \tag{2}$$

The shear viscosity is assumed to be a constant, independent of shear-strain rate. The three principal stresses in the fluid are given by the three eigenvalues of the shear-stress tensor, and are found for each point in space.[9,14] The maximum shear stress at each point in space is then given by half the difference between the two extremal principal stresses of S_{ij} at that point.[15] The uncertainty in the shear-stress measurements depends on the velocities and, more important, on the differences between adjacent velocities at the point at which the shear stress is being calculated. At the points with maximum shear stress, which are of greatest importance here, the typical velocity, and the typical change in velocity between adjacent pixels, is of the order of magnitude of 50 cm/s; these are combined, considering the error of a few percent in the velocities in each neighboring pixel, to yield a typical error of about 5% in the calculated shear stress. All the shear-stress analysis here used the Matlab toolbox (The MathWorks), and Figure 4 shows the calculated maximum shear stresses throughout the filter. The cross-shaped patterns are artifacts attributed to noise-related high-valued pixels in the velocity maps, which result in large velocity gradients and high apparent shear stresses; such artifacts can be reduced by improving the signal-to-noise ratio in the MRI velocity data.

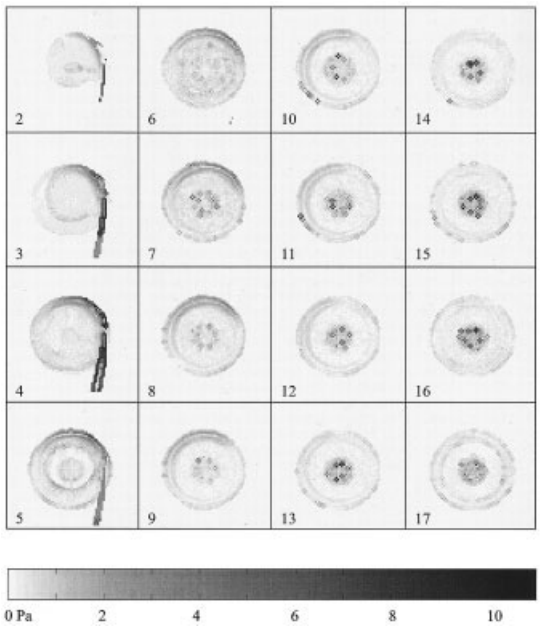

Figure 4. Shear stresses, in units of Pa, calculated from MRI velocimetry data, for the blood analogue fluid in an AL-8 filter at a flow rate of 2 L/min.

Slices 2–17 are consecutive slices across the filter from top to bottom and correspond to those shown in Figures 1 and 3. The gray scale represents maximum shear stress at each point; the highest value, of about 10 Pa, is found at the inlet.

It can be seen from Figure 4 that the maximum shear stresses, of about 10 Pa (100 dynes/cm^2), occur in the inlet region; clearly it is encouraging that this value is considerably less than the value of 150–300 Pa (1500–3000 dynes/cm^2), which is known to induce the onset of hemolysis of red blood cells.[16] The recirculatory flow pattern found is also an important observation regarding shear stress because it shows that the fluid being forced through the filter medium has a much lower velocity (0–5 cm/s) than that in either the inlet (95 cm/s) or in the main jet (80 cm/s); as a result, the fluid undergoes less severe deceleration, which for blood would further minimize potential damage to the blood cells.

Similarity to hydrocyclone flow

The flow pattern measured in this filter device is reminiscent of that which occurs in hydrocyclones used in industry for particle separation, in which the fluid is pumped, under pressure, tangentially into an inverted conical vessel, in a geometry similar to that of this blood filter, producing a spiraling fluid flow.[17,18] In hydrocyclone flow the fluid is separated into two flow paths to separate the particles suspended within the downward and upward spiraling bodies of fluid. In this blood filter, the two streams are not separated but, instead, the flow of the outer descending spiral of fluid is reversed at the base of the cylindrical vessel and becomes the inner upward going body of fluid that passes through the filter mesh into the central core of the vessel and from there to the exit port.

Comparison between MRI and computational fluid dynamics

This experimentally quantified recirculatory flow is also evident in the computational fluid dynamics (CFD) simulations of this filter system produced by PALL Medical during their design process, and summarized in Figure 5; the simulations were created using Fluent 4.3 software (Fluent USA, Lebanon, NH). Although no quantitative comparisons are made here, the qualitative agreement between the MRI measurement and CFD is clearly evident. This is an important point that is worthy of emphasis, in that this present study demonstrates the potential of MRI velocimetry as a suitable method to verify CFD simulations of fluid flow in many process engineering systems.

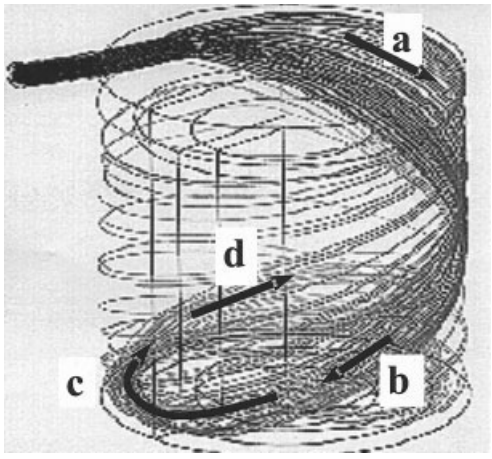

Figure 5. CFD simulation (Fluent 4.3, Fluent USA) of the flow pattern in the PALL AL8 filter, courtesy of PALL Medical.

Predicted particle paths are depicted by the lines. The recirculatory nature of the flow pattern is shown by the arrows (a)–(d), which represent the average path of the fluid. Arrow (c) shows fluid paths being reflected from the bottom of the filter vessel.

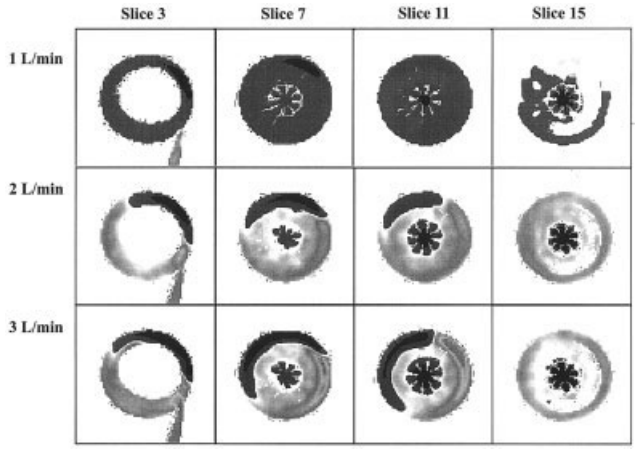

Figure 6. Four representative slices across the filter (for slice numbers refer to Figure 1) showing flow measurements at flow rates of 1, 2, and 3 L/min.

In this figure dark gray represents all downward velocities and light gray represents all upward velocities in the filter (areas of zero velocity and the area outside the filter are shown white). The recirculatory (up-welling) flow pattern appears at a flow rate between 1 and 2 L/min.

Development of recirculatory flow

Further MRI measurements at other flow rates show that this recirculatory flow pattern develops between 1 and 2 L/min. At 1 L/min, with a Reynolds number in the inlet pipe of 293, the fluid viscosity is now more important in determining the flow pattern; it causes the momentum of the inlet jet to diffuse more rapidly, which suppresses the formation of the recirculatory upward flow. Figure 6 shows flow measurements at 1, 2, and 3 L/min for representative slices across the filter, clearly demonstrating the upward recirculatory flow appearing between 1 and 2 L/min.

Summary and Conclusions

MRI velocimetry has been used to measure the flow field in an intact flow system (PALL AL8 arterial line blood filter), which is used clinically; thus the strategic implications of this study are of direct relevance to the medical devices industry. The true 3-D, noninvasive, and quantitative nature of MRI velocimetry has identified a complex, 3-D vector flow field throughout a complex geometry vessel that would have been impossible to detect using visualization techniques based on colored dyes or reflective suspended particles. These results provide insight into the trajectories followed by fluid particles entering the filter medium and, therefore, the relative usage of the filter medium; importantly, they show that at flow rates of 2 L/min and above, the fluid passing through the filter medium is part of an upward-going body of fluid. Furthermore, these data allow assessment of the shear stresses that would be

experienced by the blood cells during clinical use and show that the maximum shear stress of about 10 Pa, which occurs in the inlet port, is considerably smaller than the value of 150–300 Pa at which red cell hemolysis is induced.[16] Both are important design features. Further developments to this study will encompass the non-Newtonian behavior of real blood in the rheology of the chosen analogue fluid.

The present study was limited to flow rates of <3 L/min, which is below the 4–5.5 L/min mean operating flow rate of the filter. This was a result of the excessive fluid motion between MR excitation and MRI acquisition, which occurs at higher fluid velocities; this causes magnetically excited fluid to be outside the extent of the MR refocusing pulse, and leads to a spatially unfaithful 3-D representation of the flow field. This limitation of the specific MRI protocol used here will be addressed in future studies with MRI pulse sequences using a reduced echo time (TE) and gradient echo sequences where only one RF pulse is applied to induce the echo signal. It is expected that such studies will enable measurements of the filter at the flow rates used in clinical practice.

However, more generally, this approach to quantification of complex flow fields will be of great use to designers and researchers alike who will be able to obtain 3-D velocity measurements in flow systems of both complex geometry and with fluids that have complex rheology. Specifically, MRI offers a unique opportunity for flow measurements of any nonmetallic, intact system where the fluid and the flow vessel are transparent to radio waves; furthermore, it is capable of quantitative, on-line measurements with real fluids. There are some restrictions, however. The physical size of some flow systems may be prohibitive; thus the largest MRI scanners available are "whole-body" clinical scanners, which are based on cylindrical magnets with a bore diameter of about 1 m, or C-shaped magnets with a gap of about 60 cm; all such systems have a useful imaging field of view of about $50 \times 50 \times 50$ cm. There are other limits related to the magnetic properties of the fluid and/or suspended material and on the flow speed present; these are not discussed in depth here but further useful discussion can be found in a good text on MRI.[6-8] Importantly, MRI is able to measure the flow of optically opaque fluids, which is of particular relevance to separation and filtration of industrial slurries, as well as further studies of this filter system with whole blood.

Laser Doppler anemometry (LDA) is also a noninvasive, 3-D velocimetric measurement technique; however, it is based on scattering of laser light from seed particles (~ 10 μm) suspended in the fluid, and thus requires an optically transparent suspending fluid. LDA therefore relies on a clear optical path both into and out of the flow vessel to the point of measurement, which may not be possible for convoluted systems such as the filter investigated here; MRI has no such constraint. This study has also demonstrated that MRI velocity data can provide useful shear strain rate, and shear stress maps. MRI can also be of benefit as a means for verifying CFD models, which is of particular importance in complex geometry systems where the robustness of the CFD is strongly dependent on the suitability of the mesh constructed upon which the calculations are based. MRI and CFD offer means of mutual verification. Real measurements of rheologically complex fluids are of particular importance because modeling with viscosity functions that are nonlinear in shear strain rate is difficult, and even harder if the fluid is a multicomponent dispersion, where the computation mesh is of a size comparable with that of the dispersed particles. Finally, it may also be of interest to industry that the flow field in this blood filter is reminiscent of the flow pattern found in hydrocyclones, which are used for particle separation.

Acknowledgments

The facilities used for this study were funded by an endowment from the late Dr. Herchel Smith. It is a pleasure to acknowledge the provision of filters and stimulating support from PALL Medical, in particular Dr. Alastair Hunter and Elise Maynard; we also thank Dr. Althea de Souza for providing Figure 5.

Literature Cited

1. Kraft KA, Fatouros PP, Fei DY, Rittgers SE, Kishore PRS. MR imaging of model fluid velocity profiles. *Magn Reson Imag*. 1989;7:69-77.
2. Pope JM, Yao S. Quantitative NMR imaging of flow. *Concepts Magn Reson*. 1993;5:281-302.
3. Iwamiya JH, Chow AW, Sinton SW. NMR flow imaging of Newtonian liquids and a concentrated suspension through an axisymmetric sudden contraction. *Rheol Acta*. 1994;33:267-282.
4. Britton MM, Callaghan PT. Two-phase shear band structures at uniform stress. *Phys Rev Lett*. 1997;78:4930-4933.
5. Heese F, Hall LD. Magnetic resonance imaging (MRI) for non-invasive visualisation of filtration and separation processes. *Filtr Solutions*. 2003;3:231-236.
6. Callaghan PT. *Principles of Nuclear Magnetic Resonance Microscopy*. Oxford, UK: Clarendon Press; 1991.
7. Wehrli FW, Shaw D, Kneeland JB. *Biomedical Magnetic Resonance Imaging: Principles, Methodology, and Applications*. New York, NY: VCH; 1988.
8. McRobbie DW, Moore EA, Graves MJ, Prince MR. *MRI from Picture to Proton*. Cambridge, UK: Cambridge Univ. Press; 2002.
9. Faber TE. *Fluid Dynamics for Physicists*. Cambridge, UK: Cambridge Univ. Press; 1995.
10. Herrod NJ. *Cambridge Magnetic Resonance Software* (CaMReS). Cambridge, UK: Herchel Smith Laboratory for Medicinal Chemistry, Cambridge University; 1998.
11. Xing D, Gibbs SJ, Derbyshire JA, Carpenter TA, Hall LD. Bayesian analysis for quantitative NMR flow and diffusion imaging. *J Magn Reson*. 1995;106:1-9.
12. Bakker CJG, Bhagwandien R, Moreland MA, Fuderer M. Susceptibility artifacts in 2DFT spin echo and gradient echo imaging: The cylinder model revisited. *Magn Reson Imag*. 1993;11:539-548.
13. Sondergaard L, Stahlberg F, Thomsen C, Stensgaard A, Lindvig K, Henriksen O. Accuracy and precision of MR velocity mapping in measurements of stenotic cross-sectional area, flow rate, and pressure gradient. *J Magn Reson Imag*. 1993;3:433-437.
14. Batchelor GK. *An Introduction to Fluid Dynamics*. Cambridge, UK: Cambridge Univ. Press; 1967.
15. Hunter SC. *Mechanics of Continuous Media*. Chichester, UK: Ellis Horwood; 1983.
16. Nevaril CG, Lynch EC, Alfrey CP, Hellums JD. Erythrocyte damage and destruction induced by shearing stress. *Lab Clin Med*. 1968;71:784-790.
17. Zhao JQ, Abrahamson J. The flow in conical cyclones. Proc of 2nd Int Conf on CFD in the Minerals and Process Industries, CSIRO, Melbourne, Australia; 1999.
18. Chine B, Concha F. Flow patterns in conical and cylindrical hydrocyclones. *Chem Eng J*. 2000;80:267-273.

Manuscript received Sep. 9, 2004, and revision received Jan. 12, 2005.